Eur. Phys. J. B **8**, 389–397 (1999)

THE EUROPEAN PHYSICAL JOURNAL B

EDP Sciences

Force distribution in an inhomogeneous sandpile

J.M. Huntley[a]

Loughborough University, Department of Mechanical Engineering, Loughborough LE11 3TU, UK

Received 29 January 1998 and Received in final form 7 September 1998

Abstract. The force perturbation field in a two-dimensional pile of frictionless gravity-loaded discs or spheres arising from lattice distortions is derived to first order. The starting point is the model proposed by Liffman *et al.* (Powder Technology (1992) pp. 255-267) and Hong (Phys. Rev. E **47**, 760-762 (1993)) in which discs of uniform size are arranged on a regular lattice: this predicts a uniform normal stress distribution at the base of the pile. The analysis is applied to two problems: (i) deformable (rather than rigid) grains that undergo Hertzian deformation at the points of contact; (ii) a pile containing a gradient in particle size from the centre to the free surfaces. The former results in the classical pressure dip at the centre; the latter also produces a dip if the larger particles are at the centre.

PACS. 81.05.Rm Porous materials; granular materials – 46.10.+z Mechanics of discrete systems – 83.70.Fn Granular solids

1 Introduction

The stress analysis of granular materials has generated much interest within the physics community in recent years. This has been motivated in part by counter-intuitive experimental measurements, in particular the pressure dips observed beneath the centres of conical sandpiles [1,2]. Figure 1 shows an example from [2]. Numerical approaches [3,4] and analytical solutions [5–16] have been developed to try to explain such a phenomenon. None have so far succeeded in providing a completely satisfactory explanation from first principles. The difficulty in developing adequate theories arises for two main reasons: firstly material non-linearity (for example, the stiffness is zero in tension, non-zero in compression); and secondly the lack of a unique force distribution for a given arrangement of the grains.

The theoretical solutions fall into two main camps: continuum approaches [5–8] and microscopic models [9–16]. Of the former, the approach by Wittmer *et al.* [8], in which the orientation of the stress tensor is assumed to be constant at all points in the pile throughout the process of heap formation, has so far proved the most successful in providing solutions which are in good agreement with the available experimental data [2,8]. The microscopic models are somewhat simplistic, requiring for example the assumption of a regular lattice of grains, but can nevertheless be useful in giving exact analytical solutions which may provide insight into the more complicated real-life problem. The simplest of these is a pile of uniform smooth discs balanced on a rough floor on a regular diamond lattice [9,11,13]. This may be modified by randomness in the positions of the grains in the base [10], vacancies in the pile [14], friction [16] and the presence of horizontal contacts between grains [12]. The latter modification produced interesting results: in general terms, horizontal compressive forces generate a dip in the vertical component of force at the centre of the pile [4,12], whereas horizontal tensile forces generate a peak [15].

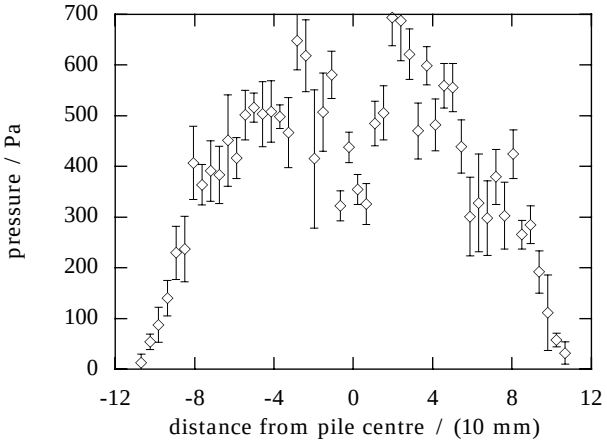

Fig. 1. Experimental force distribution along the diameter of a sandpile (average of three piles), measured from the contact diameters of a monolayer of ball bearings on silicone rubber (from [2]).

An interesting class of microscopic models which has developed recently is based on statistical rules for the transmission of force from a given grain to the supporting grains in the layer below [17–20]. Plausible assumptions for the transmission probabilities allow analytical

[a] e-mail: j.m.huntley@lboro.ac.uk

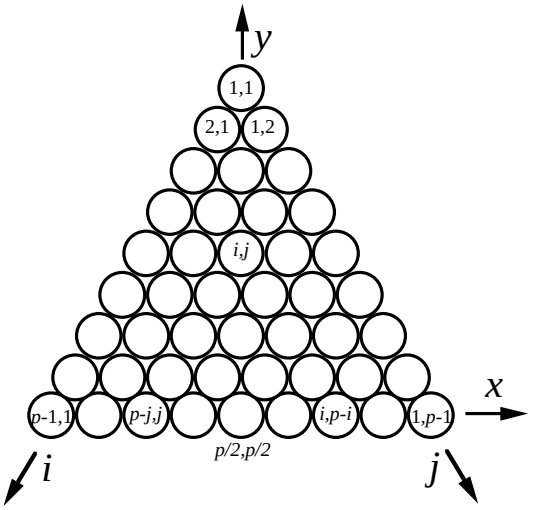

Fig. 2. Model granular pile arranged on a diamond lattice. The pile consists of $p-1$ layers ($p=10$ in this example). The support discs in the lowest layer are regarded as equivalent to the asperities on a rough floor.

expressions for the force probability density functions within the pile or bed to be derived. Such models predict both the large force fluctuations and the force networks that are observed experimentally [2,17]. Exact calculations for the force networks in two-dimensional arrays of frictionless discs with small random variations in diameter have also been carried out numerically [21,22]. These indicated that the force distribution was essentially homogeneous at length scales greater than about ten particle diameters, thus providing justification for the use of traditional continuum mechanics approaches.

The basic approach adopted in the present paper is to investigate the effect of small deviations from the perfect frictionless diagonal packing arrangement analysed previously [9,11,13]. Three sources of irregularity are considered: (i) statistical fluctuations in the positions of the support grains and disc diameters; (ii) elastic (Hertzian) deformation of the grain-grain contacts; and (iii) variations in particle size with position in the pile. The formulation developed in the paper allows the changes in pressure distribution for all three cases to be calculated analytically to first order in the parameter describing the perturbation. The results can therefore be viewed as providing a first step from the idealised regular sandpiles analysed recently in the literature towards the disordered sandpile encountered in real life.

The analysis is broken down into two steps. Firstly the displacement vector of each grain from its regular-lattice position (see Fig. 2), denoted by $\mathbf{r}(i,j)$, is determined as a function both of the displacement vectors of the support discs and of the disc sizes throughout the pile. Secondly, it is shown that the equations of equilibrium for disc (i,j) can be satisfied by the superposition of forces $\delta I(i,j)$ and $\delta J(i,j)$ acting along the i and j axes, respectively, which are related to the first and second derivatives of $\mathbf{r}(i,j)$ with respect to i and j. Integration of these forces from the free surfaces allows the total deviation in the vertical force component to be calculated at the base of the pile.

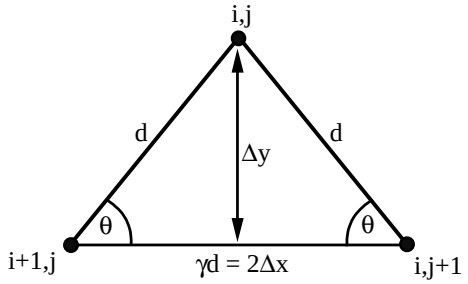

Fig. 3. Arrangement of three disc centres for the case of a regular lattice.

2 Perturbation analysis

2.1 Force distribution for the regular lattice

The starting point for the analysis is the regular-lattice model shown in Figure 2, which consists of $p-1$ layers of discs, each of diameter d. $p=10$ in this example. A non-orthogonal coordinate system (i,j) with axes along the surface diagonals will be used in the analysis. The horizontal spacing of the discs (γd: see Fig. 3) is chosen to be large enough for horizontal contacts not to occur (*i.e.*, $\gamma > 1$). The sand heap is only stable if the floor on which it is standing is rough, and thereby capable of providing a horizontal force inward to the centre of the heap. For this model, we assume the roughness to be due to asperities of the same spacing and diameter as the discs. This avoids the need for friction at the contacts. The bottom row of the pile (layer $p-1$) acts as this layer of asperities. In addition to the (i,j) coordinate system, we define a conventional Cartesian coordinate system (x,y) with its origin at the centre of the pile.

The forces acting along the i and j axes will be denoted by I and J, respectively. In the case of the regular lattice

$$I(i,j) = (i-1)W/2s \tag{1}$$
$$J(i,j) = (j-1)W/2s \tag{2}$$

are the values acting on grain (i,j) from above, where $W=mg$ is the weight of the disc (m is the mass) and s is $\sin\theta$ where θ is shown in Figure 3 [9,11,13]. The (x,y) coordinates of the centre of disc (i,j) are

$$x(i,j) = (j-i)dc \tag{3}$$
$$y(i,j) = (p-i-j)ds \tag{4}$$

where c is $\cos\theta$.

2.2 Displacement field for the irregular lattice

In this section we derive the equation for the position of each disc centre relative to that for the perfect lattice.

If Δx and Δy are used to denote the separation (in the Cartesian coordinate system) between the centres of any two nearest neighbours (see Fig. 3), then one has

$$\Delta x^2 + \Delta y^2 = d^2. \tag{5}$$

When the support discs are not uniformly spaced, and/or the discs have non-uniform diameters, then each disc is displaced from its regular-lattice position by the vector $\mathbf{r} = \big(\delta x(i,j), \delta y(i,j)\big)$. Rewriting equation (5) for discs (i,j) and $(i+1,j)$ in the irregular lattice results in

$$\begin{aligned}&[\Delta x + \delta x(i,j) - \delta x(i+1,j)]^2 \\ &\quad + [\Delta y + \delta y(i,j) - \delta y(i+1,j)]^2 = [d + \delta d_i(i,j)]^2\end{aligned} \tag{6}$$

where $\delta d_i(i,j)$ is the change in distance between the centres of the two discs. It will be assumed that $|\delta x|$, $|\delta y|$ and $|\delta d_i| \ll d$. A Taylor expansion of equation (6) then results in the following equation, valid to first order:

$$c\delta x(i,j) + s\delta y(i,j) = c\delta x(i+1,j) + s\delta y(i+1,j) + \delta d_i(i,j). \tag{7}$$

Repeating this for discs (i,j) and $(i,j+1)$ results in

$$\begin{aligned}&-c\delta x(i,j) + s\delta y(i,j) = \\ &\qquad -c\delta x(i,j+1) + s\delta y(i,j+1) + \delta d_j(i,j)\end{aligned} \tag{8}$$

where $\delta d_j(i,j)$ is the corresponding change in distance between the centres of these two discs. Addition and subtraction of equations (7, 8) allows the displacement of disc (i,j) to be expressed as follows:

$$\mathbf{r}(i,j) = \mathbf{A}\mathbf{r}(i+1,j) + \mathbf{B}\mathbf{r}(i,j+1) + \mathbf{C}(i,j) \tag{9}$$

where

$$\begin{aligned}\mathbf{A} &= \frac{1}{2}\begin{pmatrix} 1 & t \\ 1/t & 1 \end{pmatrix} \\ \mathbf{B} &= \frac{1}{2}\begin{pmatrix} 1 & -t \\ -1/t & 1 \end{pmatrix} \\ \mathbf{C}(i,j) &= \frac{1}{2cs}\begin{pmatrix} s & -s \\ c & c \end{pmatrix}\begin{pmatrix} \delta d_i(i,j) \\ \delta d_j(i,j) \end{pmatrix}\end{aligned} \tag{10}$$

and where $t = \tan\theta$. Successive application of equation (9) allows $\mathbf{r}(i,j)$ to be expressed in terms of the displacements at progressively lower layers in the pile. Going two layers down, we obtain

$$\begin{aligned}\mathbf{r}(i,j) = \mathbf{A}\mathbf{r}(i+2,j) + \mathbf{B}\mathbf{r}(i,j+2) \\ + \mathbf{A}\mathbf{C}(i+1,j) + \mathbf{B}\mathbf{C}(i,j+1) + \mathbf{C}(i,j).\end{aligned} \tag{11}$$

In deriving equation (11), the following relations were used:

$$\begin{aligned}\mathbf{A}^2 &= \mathbf{A} \\ \mathbf{B}^2 &= \mathbf{B} \\ \mathbf{A}\mathbf{B} &= \mathbf{B}\mathbf{A} = 0.\end{aligned} \tag{12}$$

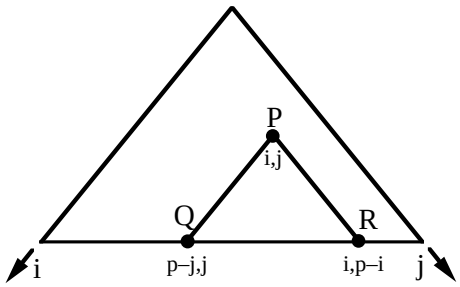

Fig. 4. Displacement vector for a disc at position P (coordinates (i,j)) from its regular-lattice position depends only on the displacement vectors of the two discs at points Q and R, together with the size deviations integrated along the lines PQ and PR.

In general one can write

$$\begin{aligned}\mathbf{r}(i,j) = \mathbf{A}\mathbf{r}(i+n,j) + \mathbf{B}\mathbf{r}(i,j+n) + \sum_{k=1}^{n-1}\mathbf{A}\mathbf{C}(i+k,j) \\ + \sum_{k=1}^{n-1}\mathbf{B}\mathbf{C}(i,j+k) + \mathbf{C}(i,j).\end{aligned} \tag{13}$$

Substitution of the value $n = p-i-j$ gives $\mathbf{r}(i,j)$ in terms of the displacements at the support discs. It is convenient for the calculations in Section 3 to replace the sums by integrals. In the interests of simplicity, we also approximate $n-1$ by n, and neglect the term $\mathbf{C}(i,j)$. The relative errors introduced by these approximations will tend to zero as $p \to \infty$. With these changes, equation (13) becomes

$$\begin{aligned}\mathbf{r}(i,j) = \mathbf{A}\mathbf{r}(p-j,j) + \mathbf{B}\mathbf{r}(i,p-i) \\ + \int_i^{p-j}\mathbf{A}\mathbf{C}(i',j)di' + \int_j^{p-i}\mathbf{B}\mathbf{C}(i,j')dj'.\end{aligned} \tag{14}$$

Once the position of the support discs has been decided, the positions of the grains in each subsequent layer are determined uniquely. If the discs are of uniform size, the two integrals are zero and equation (14) shows that the displacement of a given point (shown as P in Fig. 4) depends only on the displacement vector of discs $(p-j,j)$ and $(i,p-i)$ (Q and R, respectively, in Fig. 4). When d varies throughout the pile, the displacement vector at P also depends on the size deviations integrated along the lines PQ and PR.

2.3 Force distribution

In this section we calculate the perturbation in the regular-lattice force distribution at the base of the pile, as a result of an arbitrary displacement field, $\mathbf{r}(i,j)$. The analysis is based on satisfying the equilibrium conditions for each grain in the pile. A representative disc, (i,j), is shown in Figure 5. The contact forces are denoted by I' and J' where

$$\begin{aligned}I'(i,j) &= I(i,j) + \delta I(i,j) \\ J'(i,j) &= J(i,j) + \delta J(i,j).\end{aligned} \tag{15}$$

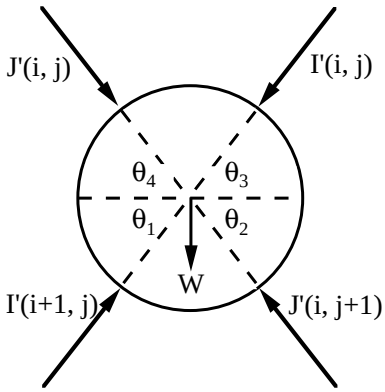

Fig. 5. Force diagram for a single disc in the pile.

The assumption that the contacts are frictionless means that the forces are all radial and cannot therefore exert any torque on the disc. The two remaining force balance equations are obtained by resolving the forces horizontally and vertically:

$$I'(i+1,j)\cos\theta_1 + J'(i,j)\cos\theta_4 - I'(i,j)\cos\theta_3 - J'(i,j+1)\cos\theta_2 = 0 \quad (16)$$

$$I'(i+1,j)\sin\theta_1 - J'(i,j)\sin\theta_4 - I'(i,j)\sin\theta_3 + J'(i,j+1)\sin\theta_2 = W \quad (17)$$

where the four angles $\theta_1, \ldots, \theta_4$ are defined in Figure 5. The corresponding equations for the regular lattice are

$$I(i+1,j)c + J(i,j)c - I(i,j)c - J(i,j+1)c = 0 \quad (18)$$

$$I(i+1,j)s - J(i,j)s - I(i,j)s + J(i,j+1)s = W. \quad (19)$$

Two simultaneous equations for the force perturbations, δI and δJ, can be obtained by substituting equation (15) into equations (16, 17), expanding the trigonometric terms to first order in $\delta\theta_k$ (where $\theta_k = \theta + \delta\theta_k$, $k = 1, 2, 3, 4$) and subtracting equations (18, 19):

$$[\delta I(i+1,j) + \delta J(i,j) - \delta I(i,j) - \delta J(i,j+1)]\,c + \big[-I(i+1,j)\delta\theta_1 - J(i,j)\delta\theta_4 + I(i,j)\delta\theta_3 + J(i,j+1)\delta\theta_2\big]s = 0 \quad (20)$$

$$[\delta I(i+1,j) - \delta J(i,j) - \delta I(i,j) + \delta J(i,j+1)]\,s + \big[I(i+1,j)\delta\theta_1 - J(i,j)\delta\theta_4 - I(i,j)\delta\theta_3 + J(i,j+1)\delta\theta_2\big]c = 0. \quad (21)$$

By taking linear combinations of equations (20, 21) and using equations (1, 2) we obtain the following recurrence relations for δI and δJ:

$$\delta I(i+1,j) = \delta I(i,j) + \frac{W}{4s^2c}\Big[(c^2-s^2)\big\{(i-1)\delta\theta_3(i,j) - i\delta\theta_1(i,j)\big\} + (j-1)\delta\theta_4(i,j) - j\delta\theta_2(i,j)\Big] \quad (22)$$

$$\delta J(i,j+1) = \delta J(i,j) + \frac{W}{4s^2c}\Big[(c^2-s^2)\big\{(j-1)\delta\theta_4(i,j) - j\delta\theta_2(i,j)\big\} + (i-1)\delta\theta_3(i,j) - i\delta\theta_1(i,j)\Big]. \quad (23)$$

In what follows, the forces acting along the j axis will not be derived directly. For a symmetrical sandpile, the δJ perturbations can be obtained from the δI values, as will be shown shortly.

The main interest is in the vertical component of the forces acting on a grain, $V'(i,j)$, $(= V(i,j) + \delta V(i,j)$, where $V(i,j)$ is the regular-lattice value and $\delta V(i,j)$ is the perturbation), which is given by

$$V'(i,j) = I'\sin\theta_3 + J'\sin\theta_4. \quad (24)$$

By expanding each term to first order in the perturbations, we obtain the i-axis contribution to $\delta V(i,j)$ as

$$\delta V_I(i,j) = \frac{Wc}{2s}\left[(i-1)\delta\theta_3\right] + s\delta I(i,j). \quad (25)$$

The perturbations in the angles $\delta\theta_1, \ldots, \delta\theta_4$ can be expressed in terms of the relative displacement vectors between the disc and its four nearest neighbours by taking scalar products with unit vectors perpendicular to the i and j axes:

$$\delta\theta_1(i,j) = \frac{1}{d}\begin{pmatrix}-s\\ c\end{pmatrix}\cdot[\mathbf{r}(i,j) - \mathbf{r}(i+1,j)] \quad (26)$$

$$\delta\theta_2(i,j) = \frac{1}{d}\begin{pmatrix}s\\ c\end{pmatrix}\cdot[\mathbf{r}(i,j) - \mathbf{r}(i,j+1)] \quad (27)$$

and by using $\delta\theta_3(i,j) = \delta\theta_1(i-1,j)$ and $\delta\theta_4(i,j) = \delta\theta_2(i,j-1)$.

Substitution of equations (26, 27) into equations (22, 25) gives the required result: the vertical force perturbations as a function of the displacement field, $\mathbf{r}(i,j)$. The term $\big\{(i-1)\delta\theta_3(i,j) - i\delta\theta_1(i,j)\big\}$ in equation (22) can be written

$$(i-1)\delta\theta_3(i,j) - i\delta\theta_1(i,j) = \frac{1}{d}\begin{pmatrix}-s\\ c\end{pmatrix}\cdot[(i-1)\mathbf{r}(i-1,j) - (2i-1)\mathbf{r}(i,j) + i\mathbf{r}(i+1,j)] \approx \frac{1}{d}\begin{pmatrix}-s\\ c\end{pmatrix}\cdot\left[\frac{\partial}{\partial i}\left(\frac{i\partial\mathbf{r}(i,j)}{\partial i}\right)\right] \quad (28)$$

where the finite difference equations

$$\frac{\partial^2\mathbf{r}(i,j)}{\partial i^2} \approx \mathbf{r}(i-1,j) - 2\mathbf{r}(i,j) + \mathbf{r}(i+1,j)$$

$$\frac{\partial\mathbf{r}(i,j)}{\partial i} \approx \mathbf{r}(i,j) - \mathbf{r}(i-1,j) \quad (29)$$

have also been used. A similar approximation for the term $(j-1)\delta\theta_4(i,j) - j\delta\theta_2(i,j)$ results in the following

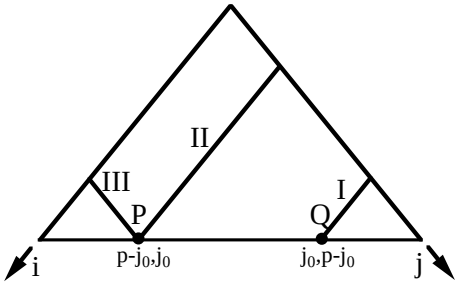

Fig. 6. The perturbations in the vertical component of force at point P can be found by carrying out the line integrals for equation (32) along paths I and II.

differential equation

$$\frac{\partial}{\partial i}\left[\delta I(i,j)\right] \approx \frac{W}{4s^2cd}\left\{(c^2-s^2)\begin{pmatrix}-s\\ c\end{pmatrix}\cdot\left[\frac{\partial}{\partial i}\left(\frac{i\partial\mathbf{r}(i,j)}{\partial i}\right)\right] + \begin{pmatrix}s\\ c\end{pmatrix}\cdot\left[\frac{\partial}{\partial j}\left(\frac{j\partial\mathbf{r}(i,j)}{\partial j}\right)\right]\right\}. \quad (30)$$

This can be integrated along a line parallel to the i axis from the free surface (at which both $\delta I(i,j)$ and i are zero) to give the force perturbation at any point in the pile:

$$\delta I(i,j) = \frac{W}{4s^2cd}\left\{(c^2-s^2)\begin{pmatrix}-s\\ c\end{pmatrix}\cdot\frac{i\partial\mathbf{r}(i,j)}{\partial i} + \begin{pmatrix}s\\ c\end{pmatrix}\cdot\int_0^i\left[\frac{\partial}{\partial j}\left(\frac{j\partial\mathbf{r}(i',j)}{\partial j}\right)\right]di'\right\}. \quad (31)$$

Finally, by combining equations (25, 26, 29, 31) we obtain the i-axis contribution to the perturbation in the vertical force component:

$$\delta V_I(i,j) = \frac{W}{4scd}\left\{-\begin{pmatrix}-s\\ c\end{pmatrix}\cdot\frac{i\partial\mathbf{r}(i,j)}{\partial i} + \begin{pmatrix}s\\ c\end{pmatrix}\cdot\int_0^i\left[\frac{\partial}{\partial j}\left(\frac{j\partial\mathbf{r}(i',j)}{\partial j}\right)\right]di'\right\}. \quad (32)$$

The j-axis contribution to $\delta V(i,j)$ can be calculated in the same way, but for piles which are symmetrical about the y axis it is easier to make use of the symmetry, as shown in Figure 6. The value of $\delta V_I(i,j)$ at point P (for which $j=j_0$, and $i=p-j$) is obtained by carrying out the line integral of equation (32) along path II. The j-axis contribution, which would require an integration along path III, can instead be obtained by evaluating $\delta V_I(i,j)$ at point Q (for which $j=p-j_0$, and $i=p-j$). The required line integral in this case is along path I.

3 Applications of the theory

3.1 Random perturbations

One possible modification to the regular lattice is the introduction of some disorder to the pile, either by random movements of the support discs, or by random changes in particle size. Let the displacement vectors of the support discs, $\mathbf{r}(p-j,j)$ be denoted $\mathbf{X}(j)$, and the deviation in diameter of disc (i,j) be denoted $Y(i,j)$. It will be assumed that the $\mathbf{X}(j)$ and $Y(i,j)$ are all independent random variables with zero means. Equation (14) shows that $\mathbf{r}(i,j)$ is a linear combination of the $\mathbf{X}(j)$ and $Y(i,j)$. Equation (32) shows that $\delta V_I(i,j)$ is a linear combination of $\mathbf{r}(i,j)$ values along the integration paths, and is therefore also a linear combination of the $\mathbf{X}(j)$ and $Y(i,j)$. By the central limit theorem, the probability density function for the $\delta V_I(i,j)$ values will therefore be approximately Gaussian with zero mean. On the average, therefore, random perturbations of the sort considered here have no effect on the pressure profiles. A similar result was found numerically by Bagster [10] for the case of random perturbations in the support disc positions. This conclusion is of course only valid for fluctuations that are small enough for second and higher order terms to be neglected. Larger fluctuations are beyond the scope of the present paper. In the two remaining applications we consider the effect of systematic changes in the disc sizes arising from both grain elasticity and polydispersity.

3.2 Effect of grain elasticity

In the simplest model (Sect. 2.1), the grains are assumed to be rigid whereas in practice they have a finite Young's modulus. Most of the deformation takes place in the region of the contact between grains. Hertzian deformation theory (see, for example, [23]) shows that

$$\delta d_i(i,j) = -\alpha\left[I(i+1,j)\right]^\beta \quad (33)$$

$$\delta d_j(i,j) = -\alpha\left[J(i,j+1)\right]^\beta \quad (34)$$

where α and β are constants associated with the grain geometry and material. For contact between two spheres of radius R, Young's modulus E and Poisson's ratio ν,

$$\alpha = \left[\frac{9(1-\nu^2)^2}{4RE^2}\right]^{1/3} \quad (35)$$

and $\beta = 2/3$. Combination of equations (10, 14, 33, 34) results in the following displacement field:

$$\mathbf{r}(i,j) = \frac{\chi}{\beta+1}\left\{\begin{pmatrix}-s\\ c\end{pmatrix}\left[(p-i)^{\beta+1}-j^{\beta+1}\right] + \begin{pmatrix}s\\ c\end{pmatrix}\left[(p-j)^{\beta+1}-i^{\beta+1}\right]\right\} \quad (36)$$

where

$$\chi = -\frac{\alpha}{2sc}\left(\frac{W}{2s}\right)^\beta. \quad (37)$$

In deriving equation (36), the displacement vectors of the support discs have all been taken to be zero. The effect of a non-zero displacement field of the supports can, if

required, be analysed separately and superposed on the solution derived in this section.

The partial derivatives of equation (36) required to calculate the force perturbations (Eq. (32)) are given by

$$\frac{i\partial \mathbf{r}(i,j)}{\partial i} = -\chi\left[\binom{-s}{c} i(p-i)^{\beta}\binom{s}{c} i^{\beta+1}\right] \quad (38)$$

$$\frac{\partial}{\partial j}\left(\frac{j\partial \mathbf{r}(i,j)}{\partial j}\right) = -\chi\Big\{\binom{-s}{c}(\beta+1)j^{\beta} + \binom{s}{c}\left[(p-j)^{\beta} - \beta j(p-j)^{\beta-1}\right]\Big\}. \quad (39)$$

Substitution of these into equation (32) results in the following expression for the force perturbations at the bottom layer of the pile:

$$\delta V_I(i,j) = \frac{-W\chi}{4scd}(p-j)\Big\{\left[\beta(c^2-s^2) - 2s^2\right] j^{\beta} + 2s^2(p-j)^{\beta} - \beta j(p-j)^{\beta-1}\Big\}. \quad (40)$$

The total vertical force perturbation at point P (Fig. 6) is obtained by summing the contributions from path I (putting $i = j_0$, $j = p - j_0$) and path II (putting $i = p - j_0$, $j = j_0$). This can then be normalised by dividing by the regular-lattice value $V = pW/2$:

$$\frac{\delta V(p-j_0, j_0)}{V} = \frac{\alpha}{2c^2 dp}\left(\frac{W}{2s}\right)^{\beta} \times\Big\{j_0^{\beta+1} + (p-j_0)^{\beta+1} - (\beta+1)\Big[(p-j_0)j_0^{\beta} + j_0(p-j_0)^{\beta}\Big]\Big\}. \quad (41)$$

This expression can be simplified further by making the following substitutions:

$$\varepsilon = \frac{2\alpha}{d}\left(\frac{Wp}{4s}\right)^{\beta} \quad (42)$$

is the fractional size change along the i-axis of the disc at coordinates $(p/2, p/2)$ due to the compression;

$$\xi = \frac{j_0 - (p/2)}{p/2} \quad (43)$$

is the normalised position under the heap ($-1 < \xi < 1$); and

$$\delta F(\xi) = \frac{\delta V(p-j_0, j_0)}{V} \quad (44)$$

is the fractional change in normal load at coordinate ξ. The result is

$$\delta F(\xi) = \frac{\varepsilon}{8c^2}\Big\{(1+\xi)^{\beta+1} + (1-\xi)^{\beta+1} - (\beta+1)\left[(1+\xi)(1-\xi)^{\beta} + (1-\xi)(1+\xi)^{\beta}\right]\Big\}. \quad (45)$$

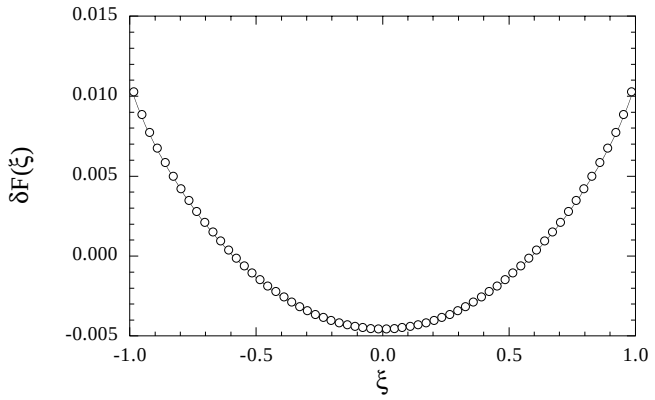

Fig. 7. Nondimensional perturbation in vertical force at base of pile due to elastic deformation at contacts ($\varepsilon = 0.01$ and $\beta = 2/3$, corresponding to Hertzian deformation for contact between spheres). Continuous line: first order analytical solution (Eq. (45)); discrete symbols: numerical solution for $p = 128$.

This is plotted in Figure 7 for the case $\varepsilon = 0.01$, $\beta = 2/3$, $\gamma = 1.2$. The results of a numerical simulation ($p = 128$) are also shown for comparison. The numerical solution involved calculating the exact displacement and force distribution fields and shows good agreement with the first order theoretical results. As a further check, it is easy to show that $\delta F(\xi)$ integrated across the base of the pile is zero. This is expected since the total weight of the pile is the same as for the case of the regular lattice.

3.3 Effect of polydispersity

If a range of particle sizes exists in the granular material, systematic variations in particle diameter with position in the pile can occur due to size segregation and stratification phenomena occurring during its formation [24]. Stratification in particular can result in strong gradients in particle size in a direction normal to the free surface. In this section we present the results of a calculation for a very simple model of such a sandpile, in which the disc diameter, d', varies linearly with distance from the nearest free surface:

$$\begin{aligned} d'(i,j) &= d + a_0 i \qquad (i < j) \\ &= d + a_0 j \qquad (i \geq j). \end{aligned} \quad (46)$$

The weights of the discs are however assumed to be identical. The distances δd_i and δd_j follow from equation (46) as

$$\begin{aligned} \delta d_i(i,j) &= (a_0/2) + a_0 i \qquad (i < j) \\ &= a_0 j \qquad (i \geq j) \\ \delta d_j(i,j) &= a_0 i \qquad (i < j) \\ &= (a_0/2) + a_0 j \qquad (i \geq j). \end{aligned} \quad (47)$$

$$\mathbf{r}(i,j) = \left(\frac{a_0}{4cs}\right)\left\{ \left[(1+2i)(p-i-j)+(p-i-j)^2\right]\begin{pmatrix} s \\ c \end{pmatrix} + 2i(p-i-j)\begin{pmatrix} -s \\ c \end{pmatrix} \right\} \qquad \text{(Zone A)}$$

$$= \left(\frac{a_0}{4cs}\right)\left\{ \left[(j-i)(1+i+j)+2j(p-2j)\right]\begin{pmatrix} s \\ c \end{pmatrix} + 2i(p-i-j)\begin{pmatrix} -s \\ c \end{pmatrix} \right\} \qquad \text{(Zone B)}$$

$$= \left(\frac{a_0}{4cs}\right)\left\{ 2j(p-i-j)\begin{pmatrix} s \\ c \end{pmatrix} + \left[(i-j)(1+i+j)+2i(p-2i)\right]\begin{pmatrix} -s \\ c \end{pmatrix} \right\} \qquad \text{(Zone C)}$$

$$= \left(\frac{a_0}{4cs}\right)\left\{ 2j(p-i-j)\begin{pmatrix} s \\ c \end{pmatrix} + \left[(1+2j)(p-i-j)+(p-i-j)^2\right]\begin{pmatrix} -s \\ c \end{pmatrix} \right\} \qquad \text{(Zone D).} \qquad (49)$$

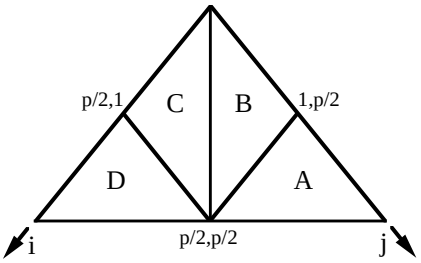

Fig. 8. Positions of the four zones required to calculate the displacement field in a model sandpile with size segregation.

The **AC** and **BC** terms required to evaluate equation (14) can then be written

$$\mathbf{AC}(i,j) = \left(\frac{a_0}{4cs}\right)(1+2i)\begin{pmatrix} s \\ c \end{pmatrix} \qquad (i<j)$$

$$= \left(\frac{a_0}{4cs}\right)(2j)\begin{pmatrix} s \\ c \end{pmatrix} \qquad (i \geq j)$$

$$\mathbf{BC}(i,j) = \left(\frac{a_0}{4cs}\right)(2i)\begin{pmatrix} -s \\ c \end{pmatrix} \qquad (i<j)$$

$$= \left(\frac{a_0}{4cs}\right)(1+2j)\begin{pmatrix} -s \\ c \end{pmatrix} \qquad (i \geq j). \qquad (48)$$

When evaluating the integrals in equation (14) the sandpile can be broken down into four zones, as shown in Figure 8. In zones A and D, paths PQ and PR (Fig. 4) do not cross the centreline, whereas in zones B and C they do and it is then necessary to break the integrals into two ranges ($i<j$ and $j \leq i$, respectively). Substitution of equation (48) into equation (14) gives the following displacement field for the four zones:

(See equation (49) above.)

As in the previous section, the displacement vectors of the support discs have all been taken to be zero.

The partial derivatives required to calculate equation (32) are listed in Table 1. Path 1 passes only through zone A, and the result is

Table 1. Partial derivatives required to evaluate equation (32) for the polydisperse sandpile.

Zone	$\begin{pmatrix} -s \\ c \end{pmatrix} \cdot \dfrac{i\dfrac{\partial \mathbf{r}(i,j)}{\partial i}}{\dfrac{a_0}{2cs}}$	$\begin{pmatrix} s \\ c \end{pmatrix} \cdot \dfrac{\dfrac{\partial}{\partial j}\left(j\dfrac{\partial \mathbf{r}(i,j)}{\partial j}\right)}{\dfrac{a_0}{2cs}}$
A	$(p-2i-j)i-(c^2-s^2)i^2$	$-(p-2j)-(c^2-s^2)i$
B	(Not required)	$p-6j-(c^2-s^2)i$
C	(Not required)	$p-i-4j-2(c^2-s^2)j$
D	$-(p-i)i-(c^2-s^2)ij$	$p-i-4j-2(c^2-s^2)j$

$$\delta V_I(i,j) = \frac{Wa_0}{8s^2c^2d}(p-j)\left[\frac{(c^2-s^2)}{2}(p-j)+j\right] \qquad (j=p/2,\ldots,p). \qquad (50)$$

Path 2 passes through zones B-D; by separating the line integral into three ranges one obtains the result

$$\delta V_I(i,j) = \frac{Wa_0}{8s^2c^2d}\left\{ -2(p-j)j - \frac{3}{2}j^2 + \frac{1}{2}(p-j)^2 + (c^2-s^2)\left[\frac{3}{2}j^2 - j(p-j)\right]\right\} \quad (j=1,2,\ldots,p/2). \qquad (51)$$

The total vertical force perturbation at point P (Fig. 6) is obtained by summing the contributions from equations (50) (putting $i=j_0$, $j=p-j_0$) and (51) (putting $i=p-j_0$, $j=j_0$):

$$\delta V(p-j_0,j_0) = \frac{Wa_0}{8s^2c^2d}\Big\{-(p-j_0)j_0 - \frac{3}{2}j_0^2 + \frac{1}{2}(p-j_0)^2 + (c^2-s^2)\left[2j_0^2 - j_0(p-j_0)\right]\Big\} \qquad (j=1,2,\ldots,p/2). \qquad (52)$$

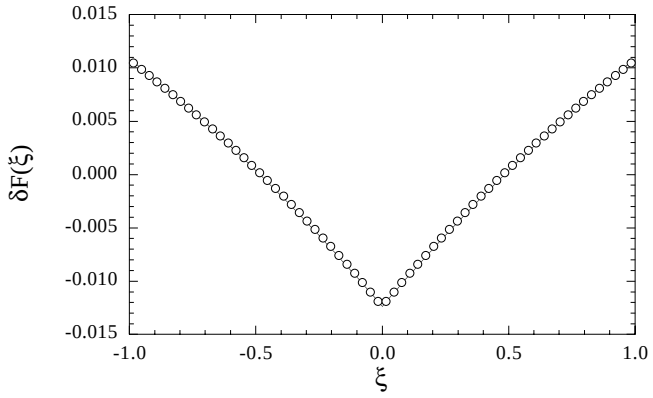

Fig. 9. Nondimensional perturbation in vertical force at base of pile due to gradient of particle sizes from the centre to the free surfaces ($\varepsilon = 0.01$). Continuous line: first order analytical solution (Eq. (53)); discrete symbols: numerical solution for $p = 128$.

In nondimensional coordinates this can be written

$$\delta F(\xi) = \frac{\varepsilon}{4\sin^2 2\theta}\big[(4\cos 2\theta - 3)(1+\xi)^2 - 2(1+\cos 2\theta)(1+\xi)(1-\xi) + (1-\xi)^2\big] \quad (-1 < \xi \le 0) \quad (53)$$

where $\delta F(-\xi) = \delta F(\xi)$ and $\varepsilon = pa_0/(2d)$ is the total fractional change in disc diameter between the surface and centre $(p/2, p/2)$ of the pile. Figure 9 shows $\delta F(\xi)$ for the case $\varepsilon = 0.01$, *i.e.* the grains at the centre are 1% larger than those at the free surfaces. There is seen to be good agreement with an exact numerical solution calculated for a pile of size $p = 128$, with $\gamma = 1.2$. The size of the pressure dip is around 1.2%, and scales in proportion to ε. As with the elastic deformation case, $\delta F(\xi)$ averages to zero over the full width of the pile.

4 Discussion

The first point to be discussed here is the case of random variations in grain size (Sect. 3.1) and the differences in the contact force patterns obtained in the present analysis as compared with those obtained by Ouaguenouni and Roux [21,22]. The starting point in the latter case was a hexagonal array of slightly polydisperse discs with, for large samples, approximately three contacts per disc. As the discs were compacted (a film of lubricant between the grains was included in the simulations as a computational device to assist in the approach to the equilibrium state), the resulting inhomogeneous force network reduced the number of active contacts to an average of 1.2 per disc, even with only small amounts of polydispersity. This contrasts with the current analysis where two non-zero contact forces are required per disc, regardless of whether the discs are monodisperse or polydisperse. The reason for this difference is that in the current case the horizontal separation of grain centres is chosen to be large enough for no horizontal contacts to occur. This constraint therefore frustrates the formation of the random force chains observed in references [21,22]. It is not clear at present what effect this constraint will have on the global stress field; the main reason for introducing it is that analytical solutions become feasible.

The pressure dip produced by grain deformation (Fig. 8) is interesting when compared with the analysis by Opie and Grindlay [15] which predicted a pressure peak for a triangular mesh of grains held together by linear springs. Substitution of the value $\beta = 1$ (corresponding to linear springs) into equation (45) still results in a pressure dip. The main differences between the two models are firstly that Opie and Grindlay allowed horizontal contacts, and secondly they assumed the floor to be smooth so that the horizontal inward forces required to stabilise the pile were provided by tension in the horizontal springs. Liffman *et al.* showed that such forces would encourage the formation of a peak rather than a dip. Tensile forces are of course not allowed in a cohesionless granular material. All the forces are compressive in the model considered in the present paper. The magnitude of the pressure reduction(around 0.5% at the centre of the pile, for a maximum grain deformation of 1%) shows that whilst this might be a significant effect for low modulus materials, it is unlikely to be the cause of the dip for most of the materials reported in experiments to date. Variations in initial grain size are a more plausible source of the necessary lattice distortions.

Previous numerical and analytical studies have already found that the introduction of polydispersity can introduce significant changes to the stress profiles [3,12]. In [12] the proposed mechanism was the introduction of horizontal contact forces. It was suggested that the small particles might lie on the lower layers: only small increases in particle diameter would then require large horizontal compressive forces in order to squeeze them onto the lattice established by the small particles. The model described in the present paper is different for several reasons: no new contacts are developed; the results are independent of the stiffness of the contacts; and a dip is produced only if the large particles are at the centre of the pile.

The latter point follows from the linear relationship between δF and the size gradient a_0 (Eq. (53)). A negative gradient will result in a force peak at the centre. When stratification occurs, the larger particles tend to ride on top of the smaller ones, causing a negative gradient within the stratum from each avalanche event. Between the strata the zones of positive gradient appear rather narrow, with almost a discontinuity in particle size [24]. If the distorted lattice breaks down across such a discontinuity, then it would appear likely that the effect of the negative gradients will dominate the force distribution, giving rise to a peak at the centre.

Size segregation is a common occurrence in avalanches, regardless of whether stratification occurs. The larger particles then tend to end up at the base of the avalanche, resulting in a positive size gradient *parallel* to the nearest free surface, unlike the size distribution assumed in equation (46). The calculations described in Section 3.3 can be

repeated for such a case and show that a positive gradient results in a pressure peak at the centre. The proposed model therefore seems unable to explain the pressure dip on the basis of commonly observed phenomena occurring during the sandpile formation.

There is, however, a simple alternative mechanism for achieving the positive gradient a_0 required to observe a pressure dip: segregation in the container from which the discs are poured. It is well known that vibration of a granular bed containing a range of grain sizes frequently results in the larger grains being preferentially positioned near the top of the bed [25]. The first particles to be poured from the container will therefore in such cases be the larger ones: these will form the centre of the pile, with progressively smaller grains lying towards the free surfaces. If segregation prior to pouring is indeed an important influence, it would be easy to verify experimentally.

5 Conclusions

The force transmission properties of simple regular-lattice models of granular materials have been extended to include the effect of small inhomogeneities. These can arise from the displacement of one or more of the support discs and from variations in the sizes of the discs. Random perturbations cause no change in the average force distribution, at least to first order in the perturbation parameter. Two systematic perturbations have been considered: elastic deformation of the grain contacts, and size gradients arising from polydispersity of the granular material. The former produces a dip in the force distribution at the centre of the pile. However, if it only distorts the lattice, rather than allowing the possibility of new contacts forming, then the magnitude of the effect is too small to explain the dip in experimental results published to date. The latter produces a significant dip for size gradients which might be encountered in practice, provided the larger particles are at the centre of the pile. One plausible mechanism for this is size segregation prior to forming the heap.

This research was carried out as part of research contract GR/L 61781, funded by the Engineering and Physical Sciences Research Council, and Shell International Oil Products BV.

References

1. J. Smid, J. Novosad, in *Proc. of 1981 Powtech Conference*, Ind. Chem. Eng. Symp. **63**, D3/V/1-D3/V/12 (1981).
2. R. Brockbank, J.M. Huntley, R.C. Ball, J. Phys. II France **7**, 1521–1532 (1997).
3. S. Luding, Phys. Rev. E **55**, 4720–4729 (1997).
4. J. Hemmingsson, H.J. Herrman, S. Roux, J. Phys. I France **7**, 291–302 (1997).
5. S.F. Edwards, R.B.S. Oakeshott, Physica D **38**, 88–92 (1989).
6. J.-P. Bouchaud, M.E. Cates, P. Claudin, J. Phys. I France **5**, 639–656 (1995).
7. S.F. Edwards, C.C. Mounfield, Physica A **226**, 25–33 (1996).
8. J.P. Wittmer, M.E. Cates, P. Claudin, J. Phys. I France **7**, 39–80 (1997).
9. D.F. Bagster, J. Powder Bulk Solids Technol. **2**, 42–46 (1978).
10. D.F. Bagster, J. Powder Bulk Solids Technol. **6**, 1–3 (1982).
11. K. Liffman, D.Y.C. Chan, B.D. Hughes, Powder Technology **72**, 255–267 (1992).
12. K. Liffman, D.Y.C. Chan, B.D. Hughes, Powder Technology **78**, 263–271 (1994).
13. D.C. Hong, Phys. Rev. E **47**, 760–762 (1993).
14. J.M. Huntley, Phys. Rev. E **48**, 4099–4101 (1993).
15. A.H. Opie, J. Grindlay, Phys. Rev. E **55**, 724–731 (1995).
16. J. Grindlay, A.H. Opie, Phys. Rev. E **55**, 718–723 (1995).
17. C.-H. Liu, S.R. Nagel, D.A. Schecter, S.N. Coppersmith, S. Majumdar, O. Narayan, T.A. Witten, Science **269**, 513–515 (1995).
18. C. Eloy, E. Clément, J. Phys. I France **7**, 1541–1558 (1997).
19. P. Claudin, J.-P. Bouchaud, M.E. Cates, J.P. Wittmer, Phys. Rev. E **57**, 4441–4457 (1998).
20. J.E.S. Socolar, Phys. Rev. E **57**, 3204–3215 (1998).
21. S. Ouaguenouni, J.N. Roux, Europhys. Lett. **32**, 449–453 (1995).
22. S. Ouaguenouni, J.N. Roux, Europhys. Lett. **39**, 117–122 (1997).
23. K.L. Johnson, *Contact mechanics* (Cambridge University Press, 1985).
24. H.A. Makse, S. Havlin, P.R. King, H.E. Stanley, Nature **386**, 379–382 (1997).
25. J.B. Knight, H.M. Jaeger, S.R. Nagel, Phys Rev. Lett. **70**, 3728–3731 (1993).